



HAL
open science

Characterisation of the performance parameters of some new broadband glasses for Raman amplification

Clara Rivero, Kathleen Richardson, Robert Stegeman, George Stegeman, Thierry Cardinal, Evelyne Fargin, Michel Couzi

► To cite this version:

Clara Rivero, Kathleen Richardson, Robert Stegeman, George Stegeman, Thierry Cardinal, et al.. Characterisation of the performance parameters of some new broadband glasses for Raman amplification. *Glass Technology - European Journal of Glass Science and Technology Part A*, 2005, 46 (2), pp.80-84. hal-00102038

HAL Id: hal-00102038

<https://hal.science/hal-00102038>

Submitted on 13 Feb 2024

HAL is a multi-disciplinary open access archive for the deposit and dissemination of scientific research documents, whether they are published or not. The documents may come from teaching and research institutions in France or abroad, or from public or private research centers.

L'archive ouverte pluridisciplinaire **HAL**, est destinée au dépôt et à la diffusion de documents scientifiques de niveau recherche, publiés ou non, émanant des établissements d'enseignement et de recherche français ou étrangers, des laboratoires publics ou privés.

Characterisation of the performance parameters of some new broadband glasses for Raman amplification

C. Rivero,¹ K. Richardson, R. Stegeman, G. Stegeman

College of Optics and Photonics/CREOL - Florida Photonics Center of Excellence, University of Central Florida, 4000 Central Florida Blvd., Orlando, FL 32816, USA

T. Cardinal, Ev. Fargin

ICMCB (UPR 9048-CNRS), 87, Avenue du Docteur Schweitzer, 33608 PESSAC cedex, France

M. Couzi

LPCM (UMR 5803-CNRS) - University of Bordeaux I, 351 Cours de la Liberation, 33405 TALENCE cedex, France

New glasses which exhibit a broadband Raman spectral response have been prepared and characterised for their Raman cross section and gain performance. Results on three different glass compositions in the system $[(100-x)\text{NaPO}_3-x\text{Na}_2\text{B}_4\text{O}_7]:\text{TiO}_2/\text{Nb}_2\text{O}_5=1$ are summarised. The impact on the Raman properties of changing the phosphorus to boron ratio while maintaining the $\text{TiO}_2/\text{Nb}_2\text{O}_5$ molar ratio equal to one, was examined. Polarised spontaneous Raman measurements are presented, and a comparison between the experimentally obtained Raman gain coefficient and that predicted from spontaneous Raman cross section measurements is made. Results obtained show that these glasses exhibit similar or slightly higher Raman gain coefficients than that of SiO_2 , with a spectral bandwidth almost five times greater ($\sim 1300\text{ cm}^{-1}$).

The demands for high speed data communication and the expected overload of data traffic requires the existing telecom window, currently operating in the C and L bands, to expand over a wider range of wavelengths. Such expansion to broader bandwidth would provide access to an additional number of channels allowing increased transmission of optical data along the optical fibre. This in turn requires an enhanced fibre transmission window, which until recently has been limited by the water absorption peak at around $1.4\ \mu\text{m}$. However, new improvements in the fibre optic industry have led to the advent of the AllWave fibre, the first full spectrum fibre designed for optical transmission over the entire telecom window of 1260–1625 nm.⁽¹⁾

Despite these advances, as information is transmitted along the optical fibre, the data signal still becomes

depleted due to intrinsic losses in the fibre. Hence, an amplification medium is necessary to provide amplification of the signal in the network. Ideally, such a medium would amplify across the full spectral bandwidth of the signal, with minimal loss. Today, erbium doped fibre amplifiers (EDFA) are considered the primary means of amplification in existing optical networks; however, EDFAs are limited to amplification in the C and L telecom bands.⁽²⁾ This leaves Raman amplifiers as the main medium available for amplification throughout the entire telecom window, given that the amplification bandwidth and position of the gain spectrum of a Raman amplifier is determined by the pump laser.⁽³⁾

Consequently, this enhancement to the telecom window has motivated the search for new materials as Raman amplification media. These materials should possess a broadband amplification window to allow minimisation of cost and components in the optical network. In other words, the broader the spectral response of these new materials, the more channels that can be amplified using a single amplifier and pump laser. Such a configuration would make the optical network more cost efficient and the Raman amplifier more attractive to future implementation in a real optical network. Of equal importance however, are crucial factors such as the trade off between the gain coefficient and the optical losses which must be taken into consideration to provide the best figure of merit available for a candidate material and its desired application.

Taking into consideration the different attributes defined above for new candidate gain media, we have examined a series of three different glass compositions in the system $[(100-x)\text{NaPO}_3-x\text{Na}_2\text{B}_4\text{O}_7]:\text{TiO}_2/\text{Nb}_2\text{O}_5=1$ in order to address and characterise their Raman

¹ Corresponding author. Email address: crivero@mail.ucf.edu

gain response. These glasses have been selected because of their overall broadband spontaneous Raman spectral response. As will be shown, the substitution of boron for phosphorus and the ratio of these two components in the glass matrix allowed us to obtain a more uniform/flat spectral gain response that spans over 1300 cm^{-1} (~ 40 THz).

Experimental procedures

Glass making

Glasses in the system $[(100-x)\text{NaPO}_3-x\text{Na}_2\text{B}_4\text{O}_7]:\text{TiO}_2/\text{Nb}_2\text{O}_5=1$, where $x=5, 10$ and 13 mol% (see Table 1) were prepared from high purity NaPO_3 (99.99% Aldrich), $\text{Na}_2\text{B}_4\text{O}_7$ (99.99% Aldrich), TiO_2 (99.995% Alfa Aesar), and Nb_2O_5 (99.998% Cerac). The glasses were melted under an oxygen atmosphere, in platinum crucibles at a temperature of 1150°C , for 5 min. After melting, the glasses were quenched onto a preheated carbon plate, and annealed at a temperature 40°C below their glass transition temperature (T_g). Finally, the glasses were cut and optically polished.

Measurements

The thermal properties of the three different glass compositions were measured with a differential scanning calorimeter (DSC) at a rate of $10^\circ\text{C}/\text{min}$. The maximum temperature measured was 675°C , and the glass transition temperature was obtained from the inflection point of the DSC thermal curve (i.e. maximum of the derivative curve).

The density of the three different glass samples was measured by the Archimedes method in diethyl phthalate at room temperature (24°C). The accuracy of the measurement is within 0.02 g/cm^3 .

The linear refractive index of the glasses was measured using the Brewster's angle method at a wavelength of 632.8 nm. The recorded reflection signal from a lock-in amplifier was fitted using Fresnel equations. The experimental error was found to be ± 0.02 .

The linear absorption spectra of the different bulk samples were obtained using a Cary 500 Scan UV-Vis-NIR Spectrophotometer.

The polarised (VV and VH) spontaneous Raman spectra of the different bulk samples were measured using a micro-Raman setup, with an excitation wavelength of 514 nm, as described by Rivero *et al.*⁽⁴⁾ The incoming polarised laser beam was focused onto the front polished surface of the sample via a $100\times$ microscope objective, with a spatial resolution of about 2 μm . A polariser and quarter wave plate ($\lambda/4$) combination were used to select the polarisation direction (vertical, V or horizontal, H) of the scattered light. A backscattered geometry was used to collect the Raman signal, which was spectrally analysed with a spectrometer and a CCD detector, with a typical resolution of about 6 cm^{-1} . The Rayleigh line was reduced

with a holographic notch filter.

The Raman gain coefficient of the three different bulk samples, specified for the selected wavelengths (or frequency shifts), was measured using the experimental setup described by Stegeman *et al.*⁽⁵⁾ A 10 Hz repetition rate Nd:YAG laser, with an excitation wavelength of 1064 nm, producing 50 ps pulses, was used as the pump wavelength for the gain measurement. The signal (probe) beam was provided via an OPG/OPA system, with a spectral output ranging from 780 – 2300 nm. Both, the pump and probe beams were spatially and temporally overlapped in the 1 – 2 mm thick bulk sample. After the sample, a monochromator was used to filter the pump from the probe wavelength. Following the monochromator, the 45° polarised signal beam (with respect to the pump beam) was split by a polarising beam splitter and directed towards two identical germanium detectors. The parallel component (VV) of the signal (with respect to the pump) was amplified given the exponential behaviour of the Raman gain process, and was used to measure 10% gain in amplitude, while the orthogonally polarised signal (VH) was used as a calibration reference.⁽⁵⁾

Results

The glass transition temperatures (T_g), crystallisation temperatures (T_c) (where applicable), densities (ρ), and refractive indices (n) of the three different compositions of the $[(100-x)\text{NaPO}_3-x\text{Na}_2\text{B}_4\text{O}_7]:\text{TiO}_2/\text{Nb}_2\text{O}_5=1$ family examined in this project are given in Table 1. In this study, we deliberately changed the phosphorus to boron ratio whilst keeping the $\text{TiO}_2/\text{Nb}_2\text{O}_5$ molar ratio equal to one.

Notice that, going from $x=5$ – 13% (i.e. increasing the boron to phosphorus ratio), there is an increase in the glass transition temperature, and for $x=10\%$, a crystallisation event is observed in the temperature range where the thermal analysis curves were measured (up to 675°C). No crystallisation event was observed for compositions $x=5, 13\%$ as measured over this temperature range.

Table 1 also shows that as the molar percent of boron to phosphorus ratio increases (i.e. increasing x), there is an inflection of the densities and refractive indices of these glass samples. Substitution of boron to phosphorus from $x=5$ – 10% causes a decrease of the volumetric weight of the glass structure, and an increase in the refractive index; however, as we increase the boron molar percentage further to $x=13\%$, there is a further increase of the density, and a small change in the refractive index.

In addition to these changes in the physical properties, Figure 1 illustrates the linear absorption coefficient of the three bulk samples. Firstly, one can see that these glasses are transparent throughout the entire telecom window, which makes them suitable for this type of application. Secondly, one can observe a blue shift in the absorption edge of the spectra, as shown in the inset graph, for increasing boron (x) content.

Figure 2(a) illustrates the spontaneous, polarised (VV and VH) Raman spectra of the three glass compositions. The VH Raman signal has been multiplied by a

Table 1.

$[(100-x)\text{NaPO}_3-x\text{Na}_2\text{B}_4\text{O}_7]:\text{TiO}_2/\text{Nb}_2\text{O}_5=1$	Thermal analysis		ρ (g/cm^3) ± 0.02 g/cm^3	$n_{632.8}$ nm ± 0.02
	T_g ($^\circ\text{C}$)	T_c ($^\circ\text{C}$)		
$x=5\%$	433	-	2.72	1.54
$x=10\%$	459	590	2.68	1.56
$x=13\%$	468	-	2.75	1.55

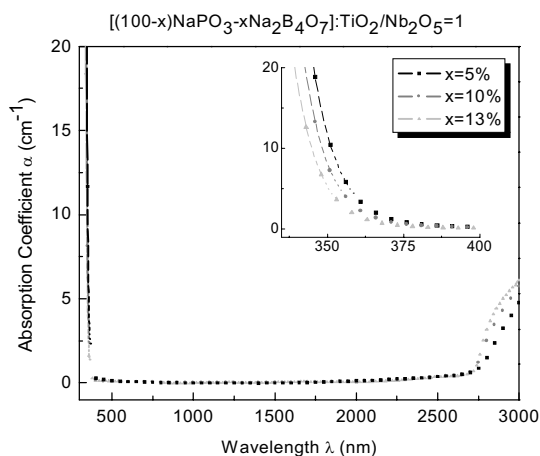


Figure 1. Absorption spectra

factor of three for comparative purposes. Since, in the majority of cases, the Raman spectrum of the glasses is highly polarisable, all the main Raman features can be obtained from the VV spectra. Due to this fact, our attention is mainly focused on the VV spectra. It is worth noticing that as the boron concentration increases (i.e. x increases), the spontaneous Raman signal becomes more polarisation dependant, given by a decrease in the intensity of the VH Raman spectra.

The spectral Raman gain coefficient was estimated using the equations described by Rivero *et al.*⁽⁴⁾ and Lines.⁽⁶⁾ A fused silica (Suprasil) sample from Heraeus and a Schott SF6 glass were used as reference calibrations using the absolute values of Raman cross section for SiO₂ and SF6 reported by Pan *et al.*⁽⁷⁾ The spontaneous Raman cross section values were obtained after correction for Fresnel losses and internal solid angle, as described by Kato & Takuma⁽⁸⁾ and Galeener.⁽⁹⁾ Figure 2(b) illustrates the spectral Raman

gain response of the three different glass samples. Note that the main contribution to the Raman gain curve is given by the Raman peak at 900 cm⁻¹. Also shown in Figure 2(b) is the experimental Raman gain coefficient obtained using the setup described by Stegeman *et al.*⁽⁵⁾ From the figure one can see that both the estimated and experimentally obtained Raman gain curves show similar spectral features. All the measurements were performed relative to the values of the spontaneous Raman cross-section and gain coefficient of fused silica at the 440 cm⁻¹ Raman vibration, given by Pan *et al.*⁽⁷⁾ and Stolen & Ippen,⁽¹⁰⁾ respectively.

Discussion

From the results obtained in Table 1, we can clearly observe that as we go from $x=10-13\%$ (corresponding to a change in the boron to phosphorus ratio of 0.44:0.60), there is clear evidence of structural reorganisation taking place in the glass matrix. This reorganisation gives rise to a transformation in the thermal stability of the glass (resulting in the emergence of a measured T_g for the $x=10\%$ sample), and an inflection point (minimum) in the density (± 0.02 g/cm³) for the same glass in the series. This reorganisation and corresponding property evolution results from a transition from a phosphate rich glass network to a borate rich network. Here these statements do not refer to any form or evidence of phase separation, but rather as an indication of which is the dominant network former in the glass. Similar results associated with such a transition have been observed in the glass system $(100-x)\text{NaPO}_3-x\text{Na}_2\text{B}_4\text{O}_7$,⁽¹¹⁾ where changes in structural configurations with variation of the B/P network were verified via NMR.⁽¹²⁾ The reorganisation in the glass structure

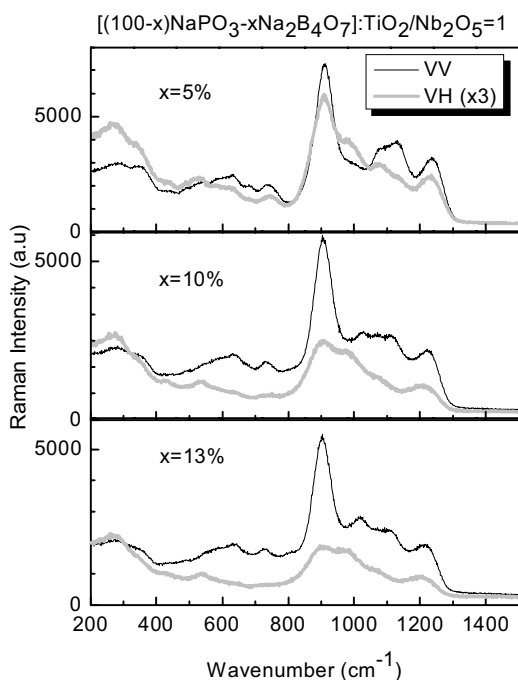


Figure 2(a). Polarised (VV and VH) spontaneous Raman spectra of glasses in the system $[(100-x)\text{NaPO}_3-x\text{Na}_2\text{B}_4\text{O}_7]:\text{TiO}_2/\text{Nb}_2\text{O}_5=1$

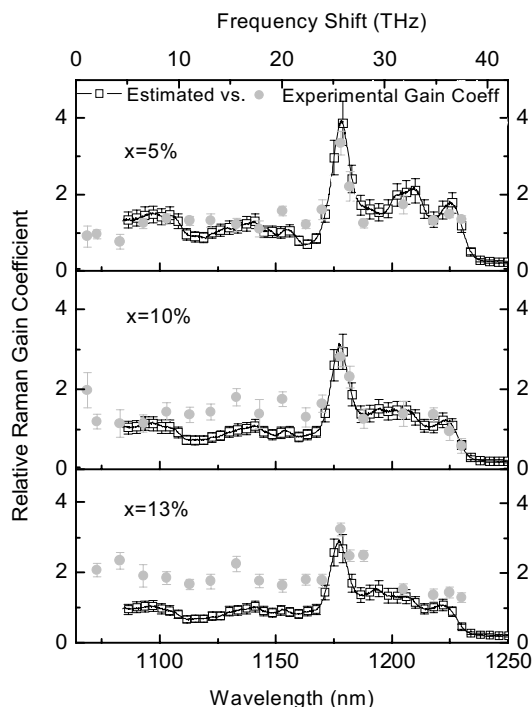


Figure 2(b). Calculated (black) and experimental (gray) Raman gain spectra of glasses in the system $[(100-x)\text{NaPO}_3-x\text{Na}_2\text{B}_4\text{O}_7]:\text{TiO}_2/\text{Nb}_2\text{O}_5=1$

has been attributed to the transformation of four coordinated boron to three coordinated boron.⁽¹²⁾ In the present study, the three coordinated boron content abruptly increases in the region where the glass network goes from a phosphate rich to borate rich (i.e. $x=10\text{--}13\%$) network, where the boron is less likely to participate in the glass matrix as linkages to the P–O–P bonds. The change in the role of the boron in the network causes the inhomogeneous introduction of titanium and niobium into the glass network, as when present in low quantities, these heavy metal species function as modifiers. Here, the introduction of titanium and niobium into the glass is more compatible for the case of a phosphate dominant network, where the less constrained network can accommodate the large ionic size of other species. These structural changes will be described in the interpretation of the Raman spectra below. Also note that the $x=10\%$ composition is less stable (important for fiberisation) since the difference between its T_x and T_g is smaller, as compared to the other two compositions.

Another essential property for this type of application is the absorption of these materials in the wavelength range of interest. Figure 1 illustrates the linear absorption curve of these three glass compositions. Note that these glasses are transparent throughout the entire telecom window. Also the inset figure shows that, as we increase the boron to phosphorus ratio (i.e. increasing x), there is a blue shift in the absorption spectra. It is important to also mention that these three particular glass compositions in the family $[(100-x)\text{NaPO}_3-x\text{Na}_2\text{B}_4\text{O}_7]:\text{TiO}_2/\text{Nb}_2\text{O}_5=1$ were chosen due to the fact that their respective parent glass network constituent exhibited the lowest OH related absorption as described by Ducal *et al.*⁽¹¹⁾ Such absorption would be detrimental to any amplifier applications.

Shown in Figure 2(a) is the polarised spontaneous Raman spectra of these three glass compositions. It can be seen that a detailed analysis of the spontaneous Raman spectra of the three glass compositions studied is very complex due to the multiple contributions of the multiple Raman active species in the glass network. The designation of the main spectral features in the spontaneous Raman spectra of borophosphate glasses in the system $(100-x)\text{NaPO}_3-x\text{Na}_2\text{B}_4\text{O}_7$ have been fully described elsewhere.⁽¹³⁾ Additionally, the Raman spectra of two similar glass families $\text{NaPO}_3-\text{Na}_2\text{B}_4\text{O}_7-\text{TiO}_2$ and $\text{NaPO}_3-\text{Na}_2\text{B}_4\text{O}_7-\text{Nb}_2\text{O}_5$ have been investigated by Cardinal *et al.*^(14,15) Using these data, we can identify the main Raman bands given in Figure 2(a). Specifically, the main phosphate vibrations observed at around 685, 1014, 1170, and 1250 cm^{-1} , have been attributed to the symmetric and asymmetric P–O–P chain vibrations, and symmetric and asymmetric stretching modes of PO_2 entities, respectively. Note that no strong boron Raman bands are noticeable in the spectra since their respective Raman vibrations are convolved within the strong Raman bands for the other glass constituents. In addition to these bands, one can clearly observe a strong Raman vibration at 900 cm^{-1} , which is attributed to the vibration of the nonbonding Nb–O short bond, found in iso-

lated NbO_6 octahedral units. Convolved within this band is also the Ti–O short bond Raman band at around 930 cm^{-1} . Other notable Raman signatures can be seen for features at 640–650, 740, and 830 cm^{-1} , which correspond to the symmetric NbO_6 and/or TiO_6 octahedral vibrations, and distorted Ti–O–Ti, and Nb–O–Nb chain vibrations, respectively. The low frequency ($<400 \text{ cm}^{-1}$) vibrations are associated with the vibrations of the heavy metal cations (i.e. Ti^{+4} and Nb^{+5}).⁽¹⁶⁾

Figure 2(b) shows the Raman spectral gain curve calculation for the three bulk samples (black), determined from the absolute spontaneous, polarised Raman intensity measurements illustrated in Figure 2(a). Note however, that the estimation of the spontaneous Raman cross section is more complex and hence less accurate ($\pm 15\%$) in this glass system, as compared to the calculations presented in our previous work on tellurite glass systems.⁽⁴⁾ We attribute this slight increase in error to the complexity of the glass system, where there are multiple contributions from the different glass constituents to a particular Raman band, all of the same order of magnitude, providing a continuous Raman bandwidth. This is in contrast to earlier results⁽⁴⁾ on tellurites where only one glass constituent (TeO_2) dominated the gain response and cross section could be predicted and measured. Consequently, the individual deconvolution of the Raman spectral features of each constituent is required to provide better agreement between the calculated spectral Raman gain response, from the spontaneous measurements, and the experimentally obtained Raman gain coefficients, due in large part to the incoherent nature of the spontaneous Raman process as compared to stimulated Raman. Such detailed deconvolution has not been performed here.

Nonetheless, from the estimated Raman gain curve response one can clearly observe that the main spontaneous Raman spectral features are still present in the Raman gain spectra, provided the appropriate Bose-Einstein correction factor for the spontaneous spectra is used.⁽¹⁷⁾ It is also evident in Figure 2(b) that the greatest contribution to the gain coefficient is given by the Raman peak at 900 cm^{-1} , which is attributed to the isolated NbO_6 octahedral vibration. This was expected since previous work^(14–16) has shown that d^0 metal ions such as Ti^{+4} , Nb^{+5} , and W^{+6} are highly polarisable. A small enhancement of the gain coefficient at this particular vibration, was observed for the glass composition with $x=5\%$ (i.e. largest phosphorus to boron ratio), since, as previously discussed, a phosphate network is more acceptable to the introduction of the d^0 ions, giving rise to a slight increase in the number density of titanium and niobium species that can be accommodated within the glass network. One can also notice however, that the overall Raman gain response for this composition ($x=5\%$) is less uniform over the spectral range shown, as characterised by the gain coefficient in the low (up to 1170 nm), peak (1180 nm), and high (>1180 nm) regimes. As previously noted, as the boron concentration in the glass is increased, the glass network structure depolymerises (due to the above mentioned boron structural re-arrangement), giving rise to a more uniform, flat Raman gain spectral re-

sponse, which is more desirable for broadband amplification applications.

Finally, the experimentally obtained Raman gain coefficients are also illustrated in Figure 2(b), and they show good agreement with the spectral gain data calculated from the spontaneous cross section measurements; the same spectral features are seen (within the experimental errors of both techniques). A measurable discrepancy between the experimental and predicted gain spectrum is observed in the low wavelength region, most notably for the $x=13\%$ sample. No explanation for this observation can be presented at this point; however, there should not be any signs of resonance enhancement at the wavelengths where these measurements were performed, given that both calculations were performed far away from the absorption edge of the sample (Figure 1). Further analysis is being undertaken to account for this discrepancy between the two results. Nonetheless, the Raman gain curves shown in Figure 2(b) reveal that the gain response of these glasses is of the same order of magnitude as fused silica, with an improved spectral bandwidth of about 40 THz, an increase in bandwidth of more than five times as compared to SiO_2 .

Conclusions

This paper presents Raman gain performance results on glasses within the system $[(100-x)\text{NaPO}_3-x\text{Na}_2\text{B}_4\text{O}_7]:\text{TiO}_2/\text{Nb}_2\text{O}_5=1$, with $x=5, 10$ and 13% .

Results show that there is an inflection of the density and linear refractive index, as the glass composition moves from a phosphorus rich to a boron rich network. This network transformation also impacts the thermal stability of the glass, with the $x=10\%$ composition exhibiting the least stability as regards fiberisation. Analysis shows that a structural transition similar to that seen in glasses without Ti/Nb occurs which exhibits a slight decrease in glass stability for $x=10\%$ composition.

From the polarised spontaneous Raman data we were able to obtain qualitative information regarding the glass structure, and estimations of the spectral gain curve for these three different glass compositions, based on spontaneous cross section measurements. Our estimations show that these glasses exhibit an overall spectral gain of the same order of magnitude as fused silica, with an improved spectral bandwidth that spans, continuously, over 1000 cm^{-1} , corresponding to 50 THz of

spectral bandwidth available for amplification applications (when pumped at 1064 nm), an improvement of almost five times as compared with SiO_2 .

Acknowledgment

This work was carried out with the support of a number of research, equipment, and educational grants, including NSF grants ECS-0123484, ECS-0225930, INT-0129235, NSF IGERT grant DGE-0114418, and NSF-CNRS grant 13050. The authors acknowledge the assistance and support of our collaborators at ICMCB / LPCM, and the School of Optics / CREOL, as well as the financial support offered by the UCF Graduate Studies office and the Student Government Association (SGA). Also, special thanks to Schott North America-Regional R & D for providing us with the SF6 glass sample.

References

1. Refi, J. J. Optical fibres for optical networking. *Bell Labs Tech. J.*, 1999, January-March, 246–61.
2. Desurvire, E., Erbium-doped fibre amplifiers: principles and applications. John Wiley & Sons, Inc., Hoboken, New Jersey, 2002.
3. Islam, M. N. Raman amplifiers for telecommunications. *IEEE J. Selected Topics Quant. Electron.*, 2002, **8**, (3), 548–59.
4. Rivero, C. *et al.* Quantifying Raman gain coefficients in tellurite glasses. *J. Non-Cryst. Solids*, 2004, **345&346**, 396–401.
5. Stegeman, R. *et al.* Tellurite glasses with peak absolute Raman gain coefficients up to 30 times that of fused silica. *Opt. Lett.*, 2003, **28** (13), 1126–8.
6. Lines, M. E. Raman-gain estimates for high-gain optical fibres. *J. Appl. Phys.*, 1987, **62** (11), 4363–70.
7. Pan, Z. *et al.* Raman scattering cross-section and nonlinear optical response of lead borate glasses. *J. Non-Cryst. Solids*, 1995, **185**, 127–34.
8. Kato, Y. & Takuma, H. Absolute measurement of Raman scattering cross-sections of liquids. *J. Opt. Soc. Am.*, 1971, **61** (3), 347–50.
9. Galeener, F. L. *et al.* The relative Raman cross sections of vitreous SiO_2 , GeO_2 , B_2O_3 , and P_2O_5 . *Appl. Phys. Lett.*, 1978, **32** (1) 34–6.
10. Stolen, R. H. & Ippen, E. P. Raman gain in glass optical waveguides. *Appl. Phys. Lett.*, 1973, **22**, (6), 276–8.
11. Duce, J. F. *et al.* Physical and chemical characterisations of sodium borophosphate glasses. *Mater. Lett.*, 1992, **13** (4–5), 271–4.
12. Duce, J. F. *et al.* ^{31}P MAS and ^{11}B NMR study of sodium rich borophosphate glasses. *Phys. Chem. Glasses*, 1994, **35** (1), 10–16.
13. Duce, J. F. *et al.* Structural study of borophosphate glasses by Raman and infrared spectroscopy. *Phys. Chem. Glasses*, 1993, **34** (5), 212–18.
14. Cardinal, T. *et al.* Raman scattering and XAFS study of optically nonlinear glasses of the $\text{TiO}_2\text{-NaPO}_3\text{-Na}_2\text{B}_4\text{O}_7$ system. *J. Solid State Chem.*, 1995, **120**, 151–6.
15. Cardinal, T. *et al.* Correlation between structural properties of $\text{Nb}_2\text{O}_5\text{-NaPO}_3\text{-Na}_2\text{B}_4\text{O}_7$ glasses and nonlinear optical activities. *J. Non-Cryst. Solids*, 1997, **222**, 228–34.
16. Miller, A. E. *et al.* The intensity of Raman scattering in glasses containing heavy metal oxides. *J. Non-Cryst. Solids*, 1988, **99**, 289–307.
17. Stolen, R. H. Issues in Raman gain measurements. *Tech. Dig. Symp. Optical Fibre Measurements*, NIST Special Publication 953 (National Institute of Standards and Technology), Gaithersburg, MD, 2000, 139–142.